Accepted Manuscript

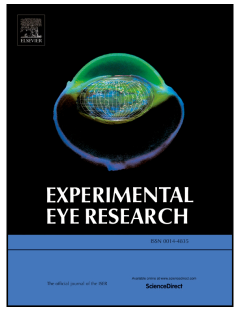

Fibronectin regulates the self-renewal of rabbit limbal epithelial stem cells by stimulating the Wnt11/Fzd7/ROCK non-canonical Wnt pathway

Mingyue Zheng, Chenglei Tian, Tingjun Fan, Bin Xu

PII: S0014-4835(18)30881-9

DOI: https://doi.org/10.1016/j.exer.2019.05.021

Reference: YEXER 7681

To appear in: *Experimental Eye Research*

Received Date: 3 December 2018

Revised Date: 23 April 2019

Accepted Date: 26 May 2019

Fibronectin regulates the self-renewal of rabbit limbal epithelial stem cells by stimulating the Wnt11/Fzd7/ROCK non-canonical Wnt pathway

Mingyue Zheng[a], Chenglei Tian[a,b], Tingjun Fan[a], Bin Xu[a,*]

[a] College of Marine Life Sciences, Ocean University of China, Qingdao, Shandong 266003, China.

[b] College of Life Sciences, Nankai University, Tianjin 300071, China.

[*] Correspondence: Bin Xu, Laboratory for Corneal Tissue Engineering, College of Marine Life Sciences, Ocean University of China, 5 Yushan Road, Qingdao 266003, Shandong Province, China. Tel.: +86 532 82031793. Fax: +86 532 82031793. E-mail address: bxu@ouc.edu.cn.

Abbreviations: ABCG2, ATP-binding cassette sub-family G member 2; CK3, cytokeratin 3; ECM, extracellular matrix; FN, fibronectin; FN-Kd, fibronectin-knockdown; Fzd, frizzled; rLESC, rabbit limbal epithelial stem cell; ROCK, Rho-associated kinase; shRNA, short hairpin RNA; siRNA, small interfering RNA.

ABSTRACT

Microenvironmental factors regulate stem cell fate. Fibronectin (FN), a key extracellular matrix component of the microenvironment, has been linked to various stem cell behaviors. However, how FN controls self-renewal, proliferation, and homeostasis of limbal stem cells remains unclear. Our study investigated the roles of FN in the self-renewal of rabbit limbal epithelial stem cells (rLESCs) by assessing rLESC proliferation and stemness in the presence and absence of FN. We further examined the effect of FN on non-canonical Wnt signaling during rLESC proliferation by evaluating the expression of cell cycle regulators. We found that rLESC proliferation increased after FN treatment and that 12.5 μg/cm^2 FN maintained rLESC stemness. FN facilitated rLESC self-renewal by promoting Wnt11 and Fzd7 interaction. Furthermore, FN modulated cell cycle regulators to enhance rLESC proliferation via the upregulation of ROCK1 and ROCK2. Our study provides new insights into the mechanism through which FN regulates the self-renewal of rLESCs; specifically, this occurs via stimulation of the Wnt11/Fzd7/ROCK non-canonical Wnt pathway. The roles of FN in the self-renewal of limbal epithelial stem cells should be further investigated for the potential treatment of limbal deficiency.

Keywords: fibronectin, self-renewal, limbal epithelial stem cell, non-canonical Wnt pathway

1. Introduction

Limbal epithelial stem cells (LESCs) are located within limbal crypts between the palisades of Vogt in the limbus (Shortt et al., 2007). Corneal epithelial cells are constantly replenished by LESCs through proliferation, differentiation, and centripetal migration. The dynamic characteristics and regenerative capacity of the corneal epithelium are critical for maintaining its structure and function during both homeostasis and wound healing (Richardson et al., 2016).

The limbus provides a unique niche for LESCs, with a microenvironment that is essential for LESC development and maintenance (Davanger and Evensen, 1971). It has been shown that limbal stroma (limbal niche) modulates epithelium in the direction favoring stemness, whereas the corneal stroma promotes differentiation (Espana et al., 2003). Moreover, outgrowths from limbal stromas showed a steady decline in a wide range of stem cell properties with distance from the central stroma, which supported the importance of proximity of stem cells to their niche environment in maintaining their undifferentiated state (Kolli et al., 2008). These results also suggest that some components of the limbal niche can maintain the properties of LESCs.

The extracellular matrix (ECM) is a dynamic microenvironment in the limbal niche that not only provides mechanical and structural support for stem cells, but also regulates cellular functions (Fuchs et al., 2004; Moore and Lemischka, 2006; Li et al., 2007; Mei et al., 2012). The ECM components collagens (III, IVα1, IVα2, and XVI), fibronectin (FN), laminin β2, vitronectin, tenascin C, SPARC, nidogen 1/2, thrombospondin 1/4, agrin, and versican are preferentially expressed in the adult limbal niche compared with their expression in the cornea (Mei et al., 2012). Thus, the specialized composition of the local ECM in the limbal niche might play a critical role in modulating cell fate decisions (Hunt et al., 2012). Indeed, it has been previously shown that hair follicle stem cells can successfully transdifferentiate into cornea-like epithelial cells in the presence of laminin-5, a major component of the cornea–limbal basement membrane zone (Blazejewska et al., 2009). And a recent study has shown that hyaluronan in the limbal stem cell niche regulates the limbal stem cell phenotype (Gesteira et al., 2017). Moreover, FN, an important ECM glycoprotein, plays an essential role in stem cell self-renewal, differentiation, migration, and adhesion (Pimton et al., 2011; Singh and Schwarzbauer, 2012; Bentzinger et al., 2013; Cheng et al., 2013; Moyes et al., 2013; Villegas et al., 2013). It has been reported that activated satellite cells dynamically remodel their niche through transient high-level expression of FN. In addition, FN can induce the symmetric expansion of satellite stem cells by enhancing Wnt7a-related signaling (Le Grand et al., 2009). Whether FN has a similar regulatory function in LESCs is unknown.

The Wnt signaling pathway, classified as canonical and non-canonical, is recognized as a dominant pathway in self-renewal and cell fate determination during embryogenesis and in stem cells of a variety of tissues (Reya and Clevers, 2005; Katoh, 2007; Nusse et al., 2008). Wnt signaling also plays an important role in the development of ocular tissues. Activation of canonical Wnt signaling promotes retina formation in mice, while expression of specific Wnt proteins and frizzled (Fzd) receptors in the lens during embryonic development reveals their function in the lens epithelium and in lens fiber differentiation (Kubo et al., 2003; Stump et al., 2003; Lyu and Joo, 2004; Das et al., 2006; Inoue et al., 2006). Wnt signaling may also regulate LESC self-renewal and differentiation. Activation of Wnt/β-catenin signaling using LiCl has been found to increase the proliferation and colony-forming efficiency of cultured human LESCs (Nakatsu et al., 2011). Moreover, several Wnt signaling components, such as Fzd7 and Wnt inhibitory factor 1, are preferentially expressed in the limbus compared with the cornea in both adult monkeys and humans (Ding et al., 2008; Nakatsu et al., 2013).

FN has been demonstrated to colocalize with Wnt receptor Fzd7 in the basal limbal epithelium layer (Mei et al., 2014). Moreover, higher FN expression has been detected in the limbus than in other areas of the cornea (Schlötzer-Schrehardt et al., 2007). In addition, our previous experiments found that FN treatment stimulated cell growth in rabbit LESCs (rLESCs). However, the molecular mechanism through which FN interacts with Wnt signaling to regulate LESC homeostasis remains unclear (Mei et al., 2014). Thus, we established FN-treatment and FN-knockdown (FN-Kd) groups to investigate the effects of FN on proliferation and stemness of rLESCs. We also studied the possible mechanisms involved in the regulation of rLESC self-renewal through the non-canonical Wnt pathway.

2. Materials and methods

2.1. Cell culture medium

rLESCs were cultured in DMEM/F12 (1:1; Cat No: 11330-032; Invitrogen, Carlsbad, CA, USA) supplemented with 10% fetal bovine serum (FBS; Cat No: 10099141; Gibco, Rockville, MD, USA), 20 ng/ml EGF (Cat No: AF-100-15; PeproTech, Rocky Hill, NJ, USA), 10 ng/ml bFGF (Cat No: AF-100-18B; PeproTech), 10 ng/ml interleukin-6 (IL-6; Cat No: AF-200-06; PeproTech), 5 μg/ml bovine insulin (Cat No: I0305000; Sigma-Aldrich, St Louis, MO, USA), 5 μg/ml siderophilin (Cat No: 41400-045; Invitrogen), 5 ng/ml sodium selenite (Cat No: 51300-044; Invitrogen), 0.5 μg/ml hydrocortisone (Cat No: 803146; Sigma-Aldrich), 30 ng/ml cholera toxin (Cat No: C8052; Sigma-Aldrich), 100 IU/ml penicillin and 100 μg/ml streptomycin (Cat No: V900929; Sigma-Aldrich).

2.2. Isolation and culturing of rLESCs

Male New Zealand rabbits (2.0–2.5 kg) without eye disease were purchased from Lukang Experimental Animal Center (Jining, Shandong, China). All animal experiments were approved by the Institutional Ethics Committee of Animal Care and Experimentation (approval no. SD-SYKY-2014-021), and were carried out in accordance with the National Institutes of Health guide for the care and use of Laboratory animals, published by the National Institutes of Health (NIH).

rLESCs were isolated from the limbal rim of New Zealand rabbit eyeballs and then cultured as described previously (Ouyang et al., 2014) with some modifications. The limbus regions were washed in phosphate buffered saline (PBS) with 100 IU/ml penicillin and 100 μg/ml streptomycin and cut into small pieces. Cell clusters were digested with 0.1% dispase II (Cat No: D4693; Sigma-Aldrich) at 37 °C for 2.5 h and then single cells were obtained by further digestion with 0.25% trypsin-EDTA (Cat No: 25200056; Thermo Fisher Scientific, Waltham, MA, USA) at 37 °C for 15 min. Primary cells were seeded on a NIH-3T3 feeder layer in 6-well plates and maintained at 37 °C and 5% CO_2 in a humidified incubator. Monoclonal stem cell growth was observed daily under an Eclipse TS100 inverted microscope (Nikon, Tokyo, Japan). And a 24-well plate was coated with 0.2% gelatin (Cat No: 1288485; Sigma-Aldrich) at 37 °C overnight, then the gelatin solution was discarded gently, leaving a gelatin-coated surface for cell culture. The monoclonal clusters were separately collected by scraping with a syringe needle under an anatomical lens and digested further using 0.25% trypsin-EDTA to isolate single cells, then seeded onto the gelatin-coated plate. The different clone clusters were cultured in different wells of the gelatin-coated plate, which was considered the second generation. And then the subsequent passage cells were directly cultured in 24-well plates without gelatin-coating. Cells at passage 5–8 were used for experiments.

2.3. rLESC treatment

2.3.1. FN treatment

rLESCs were seeded into cell culture plates coated with 12.5 μg/cm^2 FN (Cat No: F2006; Sigma-Aldrich) according to manufacturer's instructions. Briefly, FN lyophilized powder was dissolved at 1 mg/ml in sterile water. And an appropriate volume of FN solution was added into different culture plates with the final concentration of 12.5 μg/cm^2 and coated for 1 h at room temperature. Excess FN was not removed. This experimental group was termed FN(12.5).

2.3.2. FN-knockdown treatment

A short hairpin RNA (shRNA) targeting the *FN* gene was cloned into the pGPU6/Neo plasmid between the *Bam*H I and *Bbs* I restriction sites. The shRNA targeting sequence for FN-specific knockdown (FN-Kd) was as follows, 5'-CACCGCAGCACGACTTCGAACTATGTTCAAGAGACATAGTTCGAAGTCGTGCTGCT TTTTTG-3'. rLESCs were transfected using X-tremeGENE HP DNA Transfection Reagent (Cat No: 6366236001; Roche, Basel, Switzerland) according to manufacturer's instructions. The reagent (2 μl) was incubated with 1 μg plasmid DNA in 100 μl Opti-MEM I (Cat No: 31985062; Gibco) for 15 min, after which the mixture was added to the cells. Approximately 1.5 × 10^4 cells/well were seeded in a 24-well plate, which corresponded to 60–70% confluency, at the beginning of transfection. Twenty-four hours later, the cells were subjected to selection using 500 μg/ml neomycin (Cat No: N6386; Sigma-Aldrich). A pGPU6/Neo control plasmid encoding an shRNA that did not target any known genes was used as a negative control (vehicle-Kd) for knockdown experiments. The vehicle-Kd shRNA sequence was as follows, 5'-CACCGTTCTCCGAACGTGTCACGTTTCAAGAGAACGTGACACGTTCGGAGAATTTT TTG-3'.

2.3.3. Small interfering RNA (siRNA) treatment

siRNAs for *Wnt4* (siWnt4), *Wnt11* (siWnt11), *ROCK1* (siROCK1), and *ROCK2* (siROCK2) and non-targeting oligonucleotides (vehicle) were designed and synthesized by Genepharma (Shanghai, China). The siRNA sequences were as follows, siWnt4 sense, 5'-GCGCUCAUGAACCUCCAUATT-3' and antisense, 5'-UAUGGAGGUUCAUGAGCGCTT-3'; siWnt11 sense, 5'-ACAGGAUCCCAAGCCAAUATT-3' and antisense, 5'-UAUUGGCUUGGGAUCCUGUTT-3'; siROCK1 sense, 5'-CCAGAAAGGUAUAUGCUAUTT-3' and antisense, 5'-AUAGCAUAUACCUUUCUGGTT-3'; siROCK2 sense, 5'-GCAUGAAGCGGACAGGAAATT-3' and antisense, 5'-UUUCCUGUCCGCUUCAUGCTT-3'; vehicle sense, 5'-UUCUCCGAACGUGUCACGUTT-3' and antisense, 5'-ACGUGACACGUUCGGAGAATT-3'. Cells grown to a confluence of ~50% were transfected with siRNA using Lipofectamine 3000 Reagent (Cat No: L3000001; Invitrogen) according to manufacturer's instructions.

2.3.4. Treatment with ROCK inhibitor

For ROCK inhibition, rLESCs were cultured with medium containing 50 μM

N-(6-fluoro-1H-indazol-5-yl)-2-methyl-6-oxo-4-(4-(trifluoromethyl)phenyl)-1,4,5,6-tetrahydropyridine-3-carboxamide (GSK429286A; Cat No: S1474; Selleck Chemicals, Houston, TX, USA) for 48 h. rLESCs cultured without treatment were used as control.

2.4. Morphological observation

The aforementioned groups were all cultured in 24-well plates (1.5×10^4 cells/well) at 37 °C and 5% CO_2 in a humidified incubator. Growth state and morphology were separately observed and cells were counted at 3, 6, 12, and 24 h under a TS100 inverted microscope.

2.5. Cell proliferation assays

rLESCs (2,000 cells/well) of different groups were seeded in 96-well plates. Cell proliferation was assessed using Cell Counting Kit-8 (CCK-8) assays (Cat No: WST-8; Dojindo, Kumamoto, Japan) at 0, 6, 12, 18 and 24 h. Briefly, the supernatants were replaced with DMEM/F12 (1:1) medium containing 10% CCK-8 reagent. After a 2-h incubation at 37°C, the absorbance at 450 nm was measured to determine the number of viable cells, according to the manufacturer's protocol. The cell doubling time (DT) was calculated by the equation: $DT = \Delta T \times [\lg 2 / (\lg Nt - \lg N0)]$, where ΔT is the time interval, N0 is the initial cell number, and Nt is the end-point cell number.

2.6. Immunofluorescence

rLESCs (1.5×10^4 cells/well) of different groups were seeded on cell slides in 24-well plates. The culture medium was discarded after 24 h and cells were washed with PBS three times. Then, cells were fixed in 4% paraformaldehyde for 15 min and washed with PBS three times again. After permeabilizing with 0.5% Triton X-100 (prepared with PBS) for 10 min at room temperature, cells were washed with PBS three times and blocked using 2% bovine serum albumin (BSA; Cat

No: B2064; Sigma-Aldrich) at 37 °C. Next, cells were incubated with anti-ABCG2 (1:50; Cat No: ab24115; Abcam), anti-ΔNp63 (1:150; Cat No: 619001; BioLegend, San Diego, CA), anti-CK3 (1:100; Cat No: ab77869; Abcam), and anti-Ki67 (1:1000; Cat No: ab15580; Abcam) antibodies overnight at 4 °C. The cells were then washed with PBS three times and incubated with FITC-labeled secondary antibodies (Abcam) for 1 h at 37 °C. Finally, cells were counterstained with 4',6-diamidino-2-phenylindole (DAPI; Cat No: D9542; Sigma-Aldrich) for 10 min and observed under a Nikon Ti-S fluorescent microscope.

2.7. Cell cycle analysis

Flow cytometric assays were performed to analyze the cell cycle. rLESCs (4×10^5 cells/well) in 6-well plates were cultured, treated, harvested after 12 h, and fixed with 70% alcohol overnight at 4 °C. Five microliters of a 5-mg/ml propidium iodide and RNase solution (Cat No: 550825; BD Biosciences, San Jose, CA, USA) was added to 500 μl of the fixed cell suspension, followed by incubation in the dark for 30 min. The stained cells were assayed using a FACScan flow cytometer and analyzed with CXP analysis software (BD Biosciences).

2.8. RNA extraction and quantitative reverse transcription PCR (qRT-RCR)

rLESCs (4×10^5 cells/well) of different groups were seeded in 6-well plates. After 24 h, total RNA was isolated using an RNA extraction kit (Cat No: CS14010; Invitrogen) according to manufacturer's instructions and then RNA concentration was quantified using a Nanodrop 2000 (Thermo Fisher Scientific). Next cDNA was synthesized using a PrimeScript RT Reagent Kit (Cat No: RR037A; Takara, Osaka, Japan) and quantitative PCR performed using gene-specific primers and SYBR Green PCR Master Mix (Cat No: RR820A; Takara) with a Roche LightCycler 480

Real Time PCR System. The PCR cycling conditions were as follows, 95 °C for 30 s, followed by 40 cycles of 95 °C for 15 s and 60 °C for 30 s. Measurements were performed in triplicate and normalized to endogenous *GAPDH* levels. Relative fold-changes in expression were calculated using the ΔΔCT method. Primers sequences as follows, *ABCG2* sense, 5’-CAGCCTCGGTATTCCATT-3’ and antisense, 5’-TCACTGCCCTCTTCCTCT-3’; *ΔNp63* sense, 5’-GGAAAACAATGCCCAGACTC-3’ and antisense, 5’-TGCTGGAAGGACACGTCGAA-3’; *CK3* sense, 5’-GACGAAATCAACAAACGCACAG-3’ and antisense, 5’-TGGACAGCACCACGGACAT-3’; *GAPDH* sense, 5’-GTTTGTGATGGGCGTGAA-3’ and antisense, 5’-GAGGCAGGGATGATGTTCT-3’.

2.9. Luciferase assays

rLESCs treated with 12.5 μg/cm^2 FN or 20 ng/ml Wnt3a (as positive control) were seeded in 24-well plates at 1.5×10^4 cells/well. When cells reached 80–90% confluence, they were transfected with Opti-MEM containing 500 ng TCF/LEF1 luciferase reporter plasmid (Cat No: GM-021042; Genomeditech, Shanghai, China) and 1.5 μl X-tremeGENE HP DNA Transfection Reagent per well according to manufacturer’s instructions. After 24 h, the cells were lysed and luciferase activity was determined using a Dual Luciferase Kit (Cat No: TM040; Promega, Madison, WI, USA). Relative firefly luciferase activity was normalized to *Renilla* luciferase activity.

2.10. Western blot analysis

rLESCs (4×10^5 cells/well) of different groups were seeded in 6-well plates. After 24 h, cells were rinsed twice with PBS and collected after lysis with radioimmunoprecipitation assay (RIPA) buffer as total protein extract. And nuclear protein extract was prepared using NE-PER™ Nuclear and Cytoplasmic Extraction Reagents (Cat No: 78833; Thermo Fisher Scientific). Protein concentrations were quantified using the Nanodrop-2000 Spectrophotometer. Then, 25 μg of total lysate was fractionated by 10% SDS-polyacrylamide gel electrophoresis (SDS-PAGE) and further transferred onto polyvinylidene difluoride membranes (Millipore, Billerica, MA, USA). Membranes were blocked with 5% non-fat milk for 2 h at room temperature, and then incubated with primary antibodies against β-catenin (1:4000; Cat No: ab6302; Abcam), Histone H3 (1:2000; Cat No: ab1791; Abcam), ROCK1 (1:2000; Cat No: ab97592; Abcam), ROCK2 (1:5000; Cat No: 66633-1-Ig; Proteintech, Rosemont, IL, USA), cyclin D1 (1:2000; Cat No: 60186-1-Ig; Proteintech), cyclin D3 (1:500; Cat No: 26755-1-AP; Proteintech), cyclin E1 (1:500; Cat No: 11554-1-AP; Proteintech), cyclin E2 (1:500; Cat No: 11935-1-AP; Proteintech), CDK2 (1:500; Cat No: 10122-1-AP; Proteintech), CDK4 (1:500; Cat No: 11026-1-AP; Proteintech), CDK6 (1:500; Cat No: 14052-1-AP; Proteintech), $p21^{Cip1}$ (1:500; Cat No: 10355-1-AP; Proteintech), $p27^{Kip1}$ (1:1000; Cat No: 25614-1-AP; Proteintech), and GAPDH (1:5000; Cat No: 60004-1-Ig; Proteintech) at 4 °C overnight. After washing three times with TBST (TBS + 0.5% Tween-20), the samples were incubated with appropriate HRP-conjugated secondary antibodies (Abcam) for 1 h at room temperature. Immunoreactive proteins were visualized using chemilumescent (ECL) Western Blotting Substrate (Cat No: 32106; Pierce, Rockford, IL, USA) and autoradiography following manufacturer's instructions. The gray values of different proteins were analyzed using NIH Image J 1.48V software.

2.11. Co-immunoprecipitation

To detect interactions between Wnt11 and Fzd7, HEK293T cells were co-transfected with the respective pEX-3 vectors encoding Fzd7 ectodomain-HA and FLAG-tagged Wnt11 using X-tremeGENE HP DNA Transfection Reagent (Cat No: 04476093001; Roche) according to manufacturer's instructions. After 48 h, the cells were collected and resuspended in 700 μl co-IP buffer (10 mM tris-HCl pH 7.4, 100 mM NaCl, 2.5 mM $MgCl_2$, 0.5% NP-40, and 1X proteinase inhibitor), incubated on ice for 20 min, and centrifuged at 10,000 × *g* at 4 °C for 20 min. Then, 600 μl of supernatant was added to two pre-chilled Eppendorf tubes, and 10 μg of anti-FLAG antibody (Cat No: ab125243; Abcam) was added to each tube and incubated at 4 °C for 2 h. Protein A/G magnetic beads (20 μl; Cat No: sc-2003; Santa Cruz, CA, USA) were added to each tube and incubated at 4 °C overnight. And then the samples were washed with co-IP buffer. The input and eluted protein solutions were analyzed using 10% SDS-PAGE and incubated with anti-HA antibody (1:5000; Cat No: 66006-1-Ig; Proteintech) or anti-FLAG antibody at 4 °C overnight, respectively. After washing three times with TBST, the samples were incubated with goat anti-mouse HRP-conjugated secondary antibody (Cat No: ab6789; Abcam) for 1 h at room temperature. The appropriate normal immunoglobulin G (IgG) was used as a negative control.

2.12. cDNA library preparation and sequencing

A total of 3 μg RNA per sample was used as input material for RNA sample preparation of the FN(12.5), FN-Kd, and control groups. Sequencing libraries were generated using NEBNext® Ultra™ RNA Library Prep Kit for Illumina® (Cat No: E7760; NEB, Ipswich, MA, USA) following the manufacturer's recommendations and index codes were added to attribute sequences for each sample. Briefly, mRNA was purified from total RNA using poly-T oligo-attached magnetic beads. Fragmentation was carried out using divalent cations under elevated temperatures in NEBNext First Strand Synthesis Reaction Buffer. First strand cDNA was synthesized using random hexamer primers and M-MuLV Reverse Transcriptase. Second strand cDNA synthesis was subsequently performed using DNA Polymerase I and RNase H. Remaining overhangs were converted into blunt ends via exonuclease/polymerase activities. After the adenylation of the 3′ ends of DNA fragments, NEBNext Adaptor with a hairpin loop structure was ligated to prepare for hybridization. To preferentially select cDNA fragments of 250–300 bp in length, library fragments were purified using the AMPure XP system (Beckman Coulter, Brea, CA, USA). Then, 3 µl USER enzyme was used with size-selected, adaptor-ligated cDNA at 37 °C for 15 min followed by 5 min at 95 °C before PCR. PCR was performed with Phusion High-Fidelity DNA polymerase, universal PCR primers, and index (X) primer. Finally, PCR products were purified (AMPure XP system) and library quality was assessed using the Agilent Bioanalyzer 2100 system (Santa Clara, CA, USA). Raw data presented in this publication have been deposited in the Sequence Read Archive (SRA) database at NCBI under the accession number SRP152900.

2.13. Differential expression and KEGG pathway analysis

The transcript level of each expressed gene was calculated and normalized to FPKM (the number of fragments per kilobase of exon per million fragments mapped). The statistical enrichment of differentially expressed genes (DEGs) in KEGG pathways was tested between FN(12.5) and FN-Kd groups using KOBAS software. Differential expression analysis was performed using the DESeq R package (1.18.0). The heatmap was drawn by the function “pheatmap” of R package and correlation coefficients were calculation by the function “cor” in RStudio (R version 3.4.2). Corrected *p*-value of 0.05 and log2 (fold change) of 1 were set as the threshold for significantly differential expression.

2.14. Statistical analysis

Each experiment was repeated three times independently. Data were analyzed using one-way ANOVA and two-tailed *t*-tests, assuming equal variance, with SPSS 22.0 software (SPSS Inc., Chicago, IL, USA) and expressed as the mean ± standard deviation (SD). $p < 0.05$ was considered statistically significant.

3. Results

3.1. FN promotes rLESC proliferation

The number of rLESCs increased compared with that of the control group when cells were treated with different concentrations of FN (Supplemental Fig. 1A). Moreover, cells treated with FN exhibited enhanced proliferation, with 12.5 μg/cm^2 FN having the most significant effect on proliferation and maintenance of stemness (Supplemental Fig. 1B–F). Therefore, a concentration of 12.5 μg/cm^2 of FN [FN(12.5) group] was used for subsequent experiments. Moreover, two rLESC lines with FN knockdown were prepared using the shRNA targeting the *FN* gene, respectively, named FN-Kd1 and FN-Kd2. Western blot results showed that the FN expression level in the FN-Kd1 rLESCs significantly decreased by approximately 96% compared with the control, while ~57% reduction in FN-Kd2 rLESCs. Therefore, FN-Kd1 rLESCs were used for subsequent experiments and named FN-Kd rLESCs (Supplemental Fig. 2A–C).

Light microscopy analysis showed that cell numbers significantly increased in the FN(12.5) group compared with those in other groups at 3 h and 24 h. Conversely, FN-Kd rLESCs showed significantly decreased proliferation. And Annexin V staining confirmed that there was an equal number (~3%) of positive cells in the control and FN-Kd groups, suggesting that the decrease in proliferation was not due to apoptosis (Supplemental Fig. 2D). However, rLESC proliferation in the FN-Kd group was significantly enhanced after exogenous addition of FN (Fig. 1A). To quantify proliferation rate, Ki67 staining was conducted for each group, revealing that the rate of cell positivity of the FN(12.5) group was approximately 1.15–1.38-fold greater than that of the control group, which decreased to 34–72% of control levels for the FN-Kd group at different time points. Moreover, the Ki67-positive rate in the FN-Kd group after addition of exogenous FN increased by approximately 1.08–2.06-fold compared with that of the FN-Kd group. There was no significant difference in the Ki67-positive rate between the control and vehicle-Kd cells at 12 h and 24 h, though the vehicle-Kd cells showed obviously lower positive rate than control at 3 h and 6 h. These findings were consistent with the light microscopy results (Fig. 1B and C). The analysis of cell doubling times revealed that approximately 11.5±2.1 h were required by the FN(12.5) group for cell doubling, whereas the FN-Kd group required approximately 23.1±3.2 h. And the doubling time of FN-Kd rLESCs was reduced to 18.3±2.9 h after adding FN. There was no significant difference in the doubling time between the control and vehicle-Kd rLESCs, 15.2±2.2 h and 16.1±3.0 h, respectively (Fig. 1D). Furthermore, cell cycle progression was investigated in each group at 12 h and found that 53.67±3.72% of FN(12.5) rLESCs were in S phase, which was significantly higher than that of the control group (45.76±1.66%). Moreover, the proportion of cells in S phase was lowest in the FN-Kd group (23.14±0.66%), which was significantly enhanced after addition of FN (29.33±0.51%). Besides, the proportion of cells in S phase was 44.11±2.09% in the vehicle-Kd group, without significant difference from that of the control group (Fig. 2A and B).

3.2. FN upregulates the non-canonical Wnt pathway and accelerates cell cycle progression

The samples from the FN(12.5), FN-Kd, and control groups were detected for cluster analysis of DEGs (Supplemental Fig. 3). As shown in the Volcano plot, 9834 genes were detected to be differentially expressed when comparing the FN(12.5) group with the FN-Kd group, including 4894 upregulated genes (red points) and 4940 downregulated genes (green points) (Fig. 3A). These 9834 DEGs were annotated into 275 pathways, with cell cycle as the most enriched KEGG pathway. Moreover, the most enriched signaling pathways included Hippo, TNF, MAPK, mTOR, TGF-beta, VEGF, Ras, Wnt, cGMP-PKG, PI3K-Akt, Notch, NF-kappa B, and Hedgehog, as well as signaling pathways that regulate stem cell pluripotency. Genes associated with ECM-receptor interactions were also enriched in the FN(12.5) group compared with the FN-Kd group (Fig. 3B).

We then selected several genes of interest related to the Wnt signaling pathway and cell cycle. And a heatmap was generated based on expression differences at the transcription levels (Fig. 3C). Compared with the FN-Kd group, we found that *Wnt4* and *Wnt11* were significantly enhanced in the FN(12.5) group, whereas *Wnt3a*, *Wnt5a*, *Wnt5b*, *Wnt8b*, *Wnt9a*, and *Wnt10b* were significantly downregulated. In addition, *Frizzled (Fzd)-1*, *Fzd7*, and *Fzd9*, —transmembrane receptors of Wnt—were significantly upregulated in the FN(12.5) group compared with the FN-Kd group; similar expression patterns were also observed for *RhoA*, *ROCK1*, *ROCK2*, *Ror1*, *Ryk*, and *glypican 4* (*Gpc4*). In contrast, *Fzd2*, *Fzd5*, *β-catenin*, *Rac1*, and *JNK* were significantly downregulated in the FN(12.5) group. Regarding genes related to cell proliferation, we found that *CDK2*, *CDK4*, *CDK6*, *cyclin D1*, *cyclin D3*, *cyclin E1*, and *cyclin E2* were noticeably upregulated, while CDK inhibitors (CDKIs) including $p21^{Cip1}$ and $p27^{Kip1}$ were downregulated in the FN(12.5) group compared with the FN-Kd group. And the expression levels of rLESC marker *ABCG2* (Schlötzer-Schrehardt et al., 2005) and transcription factor *Myc* were also upregulated in the

FN(12.5) group compared with the FN-Kd group. Moreover, the heatmap analysis showed that *Wnt11*, *ROCK1*, *ROCK2*, *Ror1*, *Gpc4*, *cyclin D1*, *cyclin D3*, *cyclin E1*, *cyclin E2*, *CDK2*, *CDK4*, *CDK6*, *ABCG2*, and *Myc* were significantly upregulated in the FN(12.5) group compared with the control group; qRT-PCR results revealed that the scramble shRNA had no significant effects on the expressions of the genes related to the Wnt signaling (Supplemental Fig. 2E).

3.3. Wnt11 facilitates the self-renewal of rLESCs by interacting with Fzd7 to induce non-canonical Wnt signaling

Transcriptional analysis data demonstrated that *Wnt4* and *Wnt11* levels dramatically increased in the FN(12.5) group compared with the FN-Kd group. To further confirm their effects on the self-renewal of rLESCs, we independently utilized siRNAs targeting these genes. The results showed that Ki67-positivity decreased after silencing *Wnt4* expression, compared with that of the FN(12.5) group; however, this difference was not significant. Similarly, after *Wnt11* knockdown, the Ki67-positive cell rate noticeably decreased (Fig. 4A). qRT-PCR and immunostaining results suggest that inhibiting *Wnt4* and *Wnt11* expression may lead to the differentiation of rLESCs, in which CK3 was expressed abundantly while ABCG2 and ΔNp63 expressions were decreased at both the mRNA and protein levels (Fig. 4B and C).

HEK293T cells were then used to co-express FLAG-tagged Wnt11 (40 kDa) and the HA-tagged ectodomain of Fzd7 (26 kDa); co-IP results revealed that Wnt11 interacted with the ectodomain of Fzd7, confirming the interaction effects between Wnt11 and Fzd7 (Fig. 5A). Active β-catenin is known to translocate to the nucleus where it interacts with TCF/LEF1 proteins for the transcriptional activation of downstream genes during canonical Wnt signaling. Therefore, the β-catenin content in the nuclear extracts was first analyzed after treatment with FN. Nuclear β-catenin decreased by approximately 11% compared with the control level. In contrast, Wnt3a (20 ng/ml) as a positive control for nuclear translocation assays of β-catenin significantly increased (1.85 fold) the nuclear accumulation of β-catenin (Fig. 5B and C). Then the effect of β-catenin on a TCF/LEF1 luciferase reporter plasmid was examined to identify FN-induced Wnt signaling. TCF/LEF1 luciferase assays showed that FN treatment attenuated the stabilization and nuclear localization of active β-catenin in the FN(12.5) rLESCs, and the luciferase activity significantly decreased by approximately 56% compared with control levels. In contrast, Wnt3a enhanced the activation of β-catenin, yielding a 2.19-fold increase in fluorescence activity compared with that of control cells (Fig. 5D).

Moreover, RhoA, ROCK1, and ROCK2—intracellular molecules of non-canonical Wnt signaling—were all upregulated after addition of recombinant Wnt11 (10 ng/ml), whereas their expression levels were downregulated in response to siRNA-mediated targeting of *Wnt11* (Supplemental Fig. 4).

3.4. FN modulates cell cycle regulators to enhance rLESC proliferation via ROCK1 and ROCK2

Via western blotting and compared with the control group, FN was found to increase the expression of ROCK1, ROCK2, cyclin D1, cyclin D3, cyclin E1, cyclin E2, CDK2, CDK4, and CDK6, as expected; on the other hand, $p27^{Kip1}$ expression was significantly decreased. Additionally, the expression of $p21^{Cip1}$—another CDKI—was also declined, but this change was not significant (Fig. 6). To determine whether FN exerts its effect on rLESC proliferation via the ROCK signaling pathway, the specific inhibitor GSK429286A was used. Results showed that cyclin D1, cyclin D3, cyclin E1, cyclin E2, CDK2, CDK4, and CDK6 were significantly downregulated after inhibitor treatment, whereas $p21^{Cip1}$ and $p27^{Kip1}$ were obviously upregulated.

Furthermore, both siROCK1 and siROCK2 could induce the downregulation of these cyclins and CDKs as well as the upregulation of $p21^{Cip1}$ and $p27^{Kip1}$. In addition, FN treatment could not rescue the proliferation defects of rLESCs after exposure to the ROCK inhibitor or siRNA. These results suggest that FN mediates rLESC proliferation via both ROCK1 and ROCK2.

4. Discussion

FN is an important ECM glycoprotein that regulates stem cell functions including adhesion, migration, proliferation, self-renewal, and differentiation, and recent studies have demonstrated that FN shows beneficial effects on LESC proliferation, whereas other ECM components (collagen, gelatin, fibrin, etc.) are not sufficient for LESC culture (Kim et al., 2017). In the present study, we demonstrated that FN can not only increase rLESC proliferation but also maintain their stemness.

FN has been reported to affect upstream of non-canonical Wnt signaling (Le Grand et al., 2009). To further investigate the roles of FN in regulating the self-renewal of rLESCs via the non-canonical Wnt pathway, we conducted RNA-Seq analysis comparing the FN(12.5) and FN-Kd groups, and mainly focused on the enrichment of Wnt signaling and cell cycle pathways based on KEGG pathway analysis. As is known, Wnt proteins are highly secreted glycoproteins that activate the Wnt/β-catenin pathway via canonical Wnts (e.g. Wnt1, Wnt2, Wnt3a, Wnt8a, Wnt8b, Wnt10a, Wnt10b, etc.), as well as the Wnt/JNK (PCP) and Wnt/calcium pathways via non-canonical Wnts (e.g. Wnt4, Wnt5a, Wnt5b, Wnt11, etc.). Our RNA-Seq analysis revealed that transcription levels of *Wnt4* and *Wnt11* were significantly higher in the FN(12.5) group than in the FN-Kd group, whereas those of canonical Wnts were lower in the FN(12.5) rLESCs than in the FN-Kd cells.

It has been reported that Wnt4 is upregulated in fetal limbus compared with its expression in fetal central cornea (Figueira et al., 2007). Our findings demonstrated that Wnt4 suppression did not significantly decline cell proliferation; however, differentiation marker CK3 expression was significantly increased, while ABCG2 and ΔNp63—identified as the specific markers in limbal stem cells—were decreased after the rLESCs were transfected with siWnt4. Therefore, we inferred that FN may increase Wnt4 expression to maintain rLESC stemness, which still needs further study to confirm and characterize. Wnt11 is another non-canonical Wnt that is the most similar to Wnt4. Although Wnt4 and Wnt11 exhibit similar activity in some assays (Du et al., 1995), they also elicit different cellular effects (Kispert et al., 1998; Elizalde et al., 2011). In this study, we found that Wnt11 interference declines the proliferation and stemness of rLESCs; therefore, we proposed that FN can regulate rLESC self-renewal via Wnt11.

Notably, KEGG pathway analysis identified ECM-receptor interaction as one of the activated signaling pathway after FN treatment. Integrin α5β1 is the primary receptor for FN (Akiyama, 1996). The integrin receptor and enhanced FAK phosphorylation activity are upstream regulatory mechanisms that contribute to FN-mediated promotion of cell proliferation (Shroff et al., 2012). Moreover, FN has been proposed to act upstream of non-canonical Wnt signals via Syndecan 4 that binds to the heparin-binding domain of FN through its glycosaminoglycans chains to regulate integrin signaling (Woods and Couchman, 2001). Additionally, integrin-linked kinase (ILK) activation enables nuclear translocation of β-catenin by inhibiting GSK-3β activity, thus enhancing the canonical Wnt signaling (Delcommenne et al., 1998). However, the ILK expression was not upregulated in the FN(12.5) rLESCs according to our RNA-Seq data. These results suggest that integrin α5β1, probably together with Syndecan 4, mediates the effect of FN on activation of the non-canonical Wnt signaling (Muñoz et al., 2006), which needs to be further explored in rLESCs.

According to the heatmap analysis of DEGs, FN significantly enhanced the expression levels of *Fzd1*, *Fzd7*, and *Fzd9*. Furthermore, co-IP results showed that Wnt11 interacts with transmembrane Fzd7 to transmit Wnt signaling in rLESCs. Indeed, Wnt11 and Fzd7 are frequently found to interact in conjunction with other receptors including tyrosine kinase-related receptors Ror2 (Hikasa et al., 2002), Ryk (Kim et al., 2008), and heparan sulfate proteoglycan Gpc4 (Ohkawara et al., 2003). FN treatment did not affect *Ror2* expression, but upregulated *Ror1*—another Ror family receptor tyrosine kinase. In contrast to Ror2, Ror1 function in Wnt signaling has not been fully elucidated (Green et al., 2014). However, Ror1 is known to play a critical role in regulating the proliferation of satellite cells during skeletal muscle regeneration (Kamizaki et al., 2017), and has also been implicated in various non-Wnt responses (Sánchez-Solana et al., 2012). Furthermore, FN also enhanced the expression of the receptor tyrosine kinase *Ryk*, which cooperates with Fzd7 and Wnt11 during gastrulation and convergent extension movements in *Xenopus* (Kim et al., 2008; Lin et al., 2010). We also found that FN increased *Gpc4* expression in the FN(12.5) rLESCs. Additionally, the biochemical and functional interaction between Wnt11 and Fzd7 was previously found to inhibit canonical Wnt signaling mediated by Wnt3a (Uysal-Onganer and Kypta, 2012). Altogether and combined with the results of nuclear accumulation of β-catenin and luciferase reporter assays, it was revealed that FN inhibits the canonical Wnt pathway via the interaction between Wnt11 and Fzd7, and instead stimulates the non-canonical Wnt pathway in rLESCs.

Interactions between Wnt11 and Fzd7 contribute to the activation of Rho family GTPases

(Yamanaka and Nishida, 2007) and affect multiple signaling pathways that activate several different protein kinases in a cell type-specific manner (Uysal-Onganer and Kypta, 2012). Numerous studies have highlighted the importance of ROCKs in regulating cell proliferation (Croft and Olson, 2006). ROCK1 and ROCK2, exhibiting 92% identity in the kinase domain, are among the different effectors of RhoA that have been most extensively characterized. Several studies have showed differential roles for the ROCK isoforms (Yoneda et al., 2005; Yoneda et al., 2007; Lock and Hotchin, 2009; Shi et al., 2013). In the present study, RNA-Seq analysis showed that the expression levels of *RhoA*, *ROCK1*, and *ROCK2* were significantly increased after FN treatment. Moreover, upregulated RhoA, ROCK1, and ROCK2 were identified after addition of recombinant Wnt11, whereas these levels were remarkably downregulated after treatment with *Wnt11*-specific siRNA. All these findings indicate that ROCK1 and ROCK2 are involved in signaling via RhoA after enhancing the interaction between Wnt11 and Fzd7 in FN-treated rLESCs.

The precise role of ROCK in cell proliferation is not fully elucidated, and recent studies have showed that ROCK function is required for G1/S progression (Croft and Olson, 2006; Zhang et al., 2009); ROCK depletion can mediate cell cycle arrest—most likely in the G1 phase (Kümper et al., 2016). One *in vivo* study reported that over-activation of ROCK2 contributes to hyperproliferation and epidermal thickening in mouse skin (Samuel et al., 2011). The effects of ROCK activity on the levels of cell cycle regulatory proteins have also been implicated in the proliferation of corneal epithelial cells (Chen et al., 2008). Based on this evidence, we further investigated the role of ROCK in modulating the levels of specific cell cycle regulators in rLESCs.

Progression through each stage of the cell cycle requires different sets of cyclins, CDKs, and

CDKIs (Morgan, 1997). Transition through the G1 phase is regulated by CDK4/cyclin D1 and CDK6/cyclin D3. CDK2/cyclin E is active during late G1 phase and is responsible for G1/S transition. Negative regulation of CDK2 includes its association with the $p21^{Cip1}$ and $p27^{Kip1}$ inhibitory proteins (Coulonval et al., 2003). Western blot results in this study showed that expression levels of cyclin D1, cyclin D3, cyclin E1, cyclin E2, CDK2, CDK4, and CDK6 were enhanced in the FN(12.5) group, whereas those of $p21^{Cip1}$ and $p27^{Kip1}$ decreased, suggesting that the FN-treated cells could transition from G1 to S phase more quickly, decreasing cell cycle duration and increasing proliferation. After inhibiting ROCK1 and ROCK2 with GSK429286A, the cyclins and CDKs were significantly downregulated, whereas the CDKIs were upregulated. To further investigate the roles of the two ROCK isoforms, we targeted each isoform independently with siRNAs. The results revealed that ablation of either ROCK1 or ROCK2 decreased cyclin and CDK expression and increased CDKI expression. Moreover, FN addition could not rescue the proliferation defects in the rLESCs treated with either the ROCK inhibitor or siRNA because the ROCK pathway was blocked. These results indicate that FN enhances rLESC proliferation via both ROCK1 and ROCK2, and that ROCK1 and ROCK2 function redundantly.

Moreover, studies have confirmed that Myc plays an important role in promoting the self-renewal of embryonic stem cells (Fagnocchi et al., 2016). Myc is not only essential for the maintenance of epithelial stem cell homeostasis, as it also regulates the directional differentiation and proliferation of epithelial stem cells during wound healing (Honeycutt and Roop, 2004). Several studies have found that ROCK can phosphorylate Myc at threonine 58 and/or serine 62 to increase Myc stability after nuclear translocation (Liu et al., 2009; Zhang et al., 2014). Nuclear Myc also induces the expression of several positive regulators of cell cycle progression by binding to their promoters, and repress p21^{Cip1} and p27^{Kip1} activities via different mechanisms. Consequently, Myc stimulates cell cycle progression and cellular proliferation (Bretones et al., 2015). In the present study, RNA-Seq analysis demonstrated that expression levels of Myc in the FN(12.5) group were significantly higher than that of the FN-Kd group. Therefore, we theorized that ROCK may promote rLESC proliferation by increasing Myc activity, which needs to be verified in the future.

In conclusion, FN not only enhances rLESC proliferation but also maintains stemness by promoting Wnt11 and Fzd7 interactions. Moreover, rLESC proliferation is increased through ROCK1 and ROCK2 upregulation as well as further modulation of cell cycle regulators (Fig. 7). Our findings provide new evidence that FN play an important role in rLESC self-renewal via stimulation of the Wnt11/Fzd7/ROCK non-canonical Wnt pathway. FN may thus be an essential component of ECM scaffolds for limbus transplantation.

Authors' contributions

All authors participated in the research and approved the final version of the manuscript. BX supervised the project and prepared the manuscript. MZ and CT were involved in the experimental design, performance of experiments, discussion of results. TF was responsible for the analyses of the data.

Acknowledgments

The authors gratefully acknowledge Prof. Mingzhuang Zhu of the Key Laboratory of Mariculture, Ocean University of China, for their help and guidance with flow cytometric analysis. This work was supported by the National Natural Science Foundation of China [grant number 31601104].

Conflicts of interest

The authors declare no conflict of interest.

References

Akiyama, S.K., 1996. Integrins in cell adhesion and signaling. Hum. Cell 9, 181–186.

Bentzinger, C.F., Wang, Y.X., von Maltzahn, J., Soleimani, V.D., Yin, H., Rudnicki, M.A., 2013. Fibronectin regulates Wnt7a signaling and satellite cell expansion. Cell Stem Cell 12, 75–87.

Blazejewska, E.A., Schlötzer-Schrehardt, U., Zenkel, M., Bachmann, B., Chankiewitz, E., Jacobi, C., Kruse, F.E., 2009. Corneal limbal microenvironment can induce transdifferentiation of hair follicle stem cells into corneal epithelial-like cells. Stem Cells 27, 642–652.

Bretones, G., Delgado, M.D., León, J., 2015. Myc and cell cycle control. Biochim. Biophys. Acta 1849, 506–516.

Chen, J., Guerriero, E., Lathrop, K., SundarRaj, N., 2008. Rho/ROCK signaling in regulation of corneal epithelial cell cycle progression. Invest. Ophthalmol. Vis. Sci. 49, 175–183.

Cheng, P., Andersen, P., Hassel, D., Kaynak, B.L., Limphong, P., Juergensen, L., Kwon, C., Srivastava, D., 2013. Fibronectin mediates mesendodermal cell fate decisions. Development 140, 2587–2596.

Coulonval, K., Bockstaele, L., Paternot, S., Roger, P.P., 2003. Phosphorylations of cyclin-dependent kinase 2 revisited using two-dimensional gel electrophoresis. J. Biol. Chem. 278, 52052–52060.

Croft, D.R., Olson, M.F., 2006. The Rho GTPase effector ROCK regulates cyclin A, cyclin D1, and p27Kip1 levels by distinct mechanisms. Mol. Cell Biol. 26, 4612–4627.

Das, A.V., Zhao, X., James, J., Kim, M., Cowan, K.H., Ahmad, I., 2006. Neural stem cells in the adult ciliary epithelium express GFAP and are regulated by Wnt signaling. Biochem. Biophys. Res. Commun. 339, 708–716.

Davanger, M., Evensen, A., 1971. Role of the pericorneal papillary structure in renewal of corneal epithelium. Nature 229, 560–561.

Delcommenne, M., Tan, C., Gray, V., Rue, L., Woodgett, J., Dedhar, S., 1998. Phosphoinositide-3-OH kinase-dependent regulation of glycogen synthase kinase 3 and protein kinase B/AKT by the integrin-linked kinase. Proc. Natl. Acad. Sci. U S A 95, 11211–12116.

Ding, Z., Dong, J., Liu, J., Deng, S.X., 2008. Preferential gene expression in the limbus of the vervet monkey. Mol. Vis. 14, 2031–2041.

Du, S.J., Purcell, S.M., Christian, J.L., McGrew, L.L., Moon, R.T., 1995. Identification of distinct classes and functional domains of Wnts through expression of wild-type and chimeric proteins in Xenopus embryos. Mol. Cell Biol. 15, 2625–2634.

Elizalde, C., Campa, V.M., Caro, M., Schlangen, K., Aransay, A.M., Vivanco, Md., Kypta, R.M., 2011. Distinct roles for Wnt-4 and Wnt-11 during retinoic acid-induced neuronal differentiation. Stem Cells 29, 141–153.

Espana, E.M., Kawakita, T., Romano, A., Di Pascuale, M., Smiddy, R., Liu, C.Y., Tseng, S.C., 2003. Stromal niche controls the plasticity of limbal and corneal epithelial differentiation in a rabbit model of recombined tissue. Invest. Ophthalmol. Vis. Sci. 44, 5130–5135.

Fagnocchi, L., Cherubini, A., Hatsuda, H., Fasciani, A., Mazzoleni, S., Poli, V., Berno, V., Rossi, R.L., Reinbold, R., Endele, M., Schroeder, T., Rocchigiani, M., Szkarłat, Ż., Oliviero, S., Dalton, S., Zippo, A., 2016. A Myc-driven self-reinforcing regulatory network maintains mouse embryonic stem cell identity. Nat. Commun. 7, 11903.

Figueira, E.C., Di Girolamo, N., Coroneo, M.T., Wakefield, D., 2007. The phenotype of limbal epithelial stem cells. Invest. Ophthalmol. Vis. Sci. 48, 144–156.

Fuchs, E., Tumbar, T., Guasch, G., 2004. Socializing with the neighbors: stem cells and their niche. Cell 116, 769–778.

Gesteira, T.F., Sun, M., Coulson-Thomas, Y.M., Yamaguchi, Y., Yeh, L.K., Hascall, V., Coulson-Thomas, V.J., 2017. Hyaluronan rich microenvironment in the limbal stem cell niche regulates limbal stem cell differentiation. Invest. Ophthalmol. Vis. Sci. 58, 4407–4421.

Green, J., Nusse, R., van Amerongen, R., 2014. The role of Ryk and Ror receptor tyrosine kinases in Wnt signal transduction. Cold Spring Harb. Perspect. Biol. 6, a009175.

Hikasa, H., Shibata, M., Hiratani, I., Taira, M., 2002. The Xenopus receptor tyrosine kinase Xror2 modulates morphogenetic movements of the axial mesoderm and neuroectoderm via Wnt signaling. Development 129, 5227–5239.

Honeycutt, K.A., Roop, D.R., 2004. c-Myc and epidermal stem cell fate determination. J. Dermatol. 31, 368–375.

Hunt, G.C., Singh, P., Schwarzbauer, J.E., 2012. Endogenous production of fibronectin is required for self-renewal of cultured mouse embryonic stem cells. Exp. Cell Res. 16, 1820–1831.

Inoue, T., Kagawa, T., Fukushima, M., Shimizu, T., Yoshinaga, Y., Takada, S., Tanihara, H., Taga, T., 2006. Activation of canonical Wnt pathway promotes proliferation of retinal stem cells derived from adult mouse ciliary margin. Stem Cells 24, 95–104.

Kamizaki, K., Doi, R., Hayashi, M., Saji, T., Kanagawa, M., Toda, T., Fukada, S.I., Ho, H.H., Greenberg, M.E., Endo, M., Minami, Y., 2017. The Ror1 receptor tyrosine kinase plays a critical role in regulating satellite cell proliferation during regeneration of injured muscle. J. Biol. Chem. 292, 15939–15951.

Katoh, M., 2007. Networking of WNT, FGF, Notch, BMP, and Hedgehog signaling pathways during carcinogenesis. Stem Cell Rev. 3, 30–38.

Kim, E.K., Lee, G.H., Lee, B., Maeng, Y.S., 2017. Establishment of novel limbus-derived, highly proliferative ABCG2+/ABCB5+ limbal epithelial stem cell cultures. Stem Cells Int. 2017, 7678637.

Kim, G.H., Her, J.H., Han, J.K., 2008. Ryk cooperates with Frizzled 7 to promote Wnt11-mediated endocytosis and is essential for Xenopus laevis convergent extension movements. J. Cell Biol. 182, 1073–1082.

Kispert, A., Vainio, S., McMahon, A.P., 1998. Wnt-4 is a mesenchymal signal for epithelial transformation of metanephric mesenchyme in the developing kidney. Development 125, 4225–4234.

Kolli, S., Lako, M., Figueiredo, F., Mudhar, H., Ahmad, S., 2008. Loss of corneal epithelial stem cell properties in outgrowths from human limbal explants cultured on intact amniotic membrane. Regen. Med. 3, 329–342.

Kubo, F., Takeichi, M., Nakagawa, S., 2003. Wnt2b controls retinal cell differentiation at the ciliary marginal zone. Development 130, 587–598.

Kümper, S., Mardakheh, F.K., McCarthy, A., Yeo, M., Stamp, G.W., Paul, A., Worboys, J., Sadok, A., Jørgensen, C., Guichard, S., Marshall, C.J., 2016. Rho-associated kinase (ROCK) function is essential for cell cycle progression, senescence and tumorigenesis. Elife 5, e12994.

Le Grand, F., Jones, A.E., Seale, V., Scimè, A., Rudnicki, M.A., 2009. Wnt7a activates the planar cell polarity pathway to drive the symmetric expansion of satellite stem cells. Cell Stem Cell 4, 535–547.

Li, W., Hayashida, Y., Chen, Y.T., Tseng, S.C., 2007. Niche regulation of corneal epithelial stem cells at the limbus. Cell Res. 17, 26–36.

Lin, S., Baye, L.M., Westfall, T.A., Slusarski, D.C., 2010. Wnt5b-Ryk pathway provides directional signals to regulate gastrulation movement. J. Cell Biol. 190, 263–278.

Liu, S., Goldstein, R.H., Scepansky, E.M., Rosenblatt, M., 2009. Inhibition of rho-associated kinase signaling prevents breast cancer metastasis to human bone. Cancer Res. 69, 8742–8751.

Lock, F.E., Hotchin, N.A., 2009. Distinct roles for ROCK1 and ROCK2 in the regulation of keratinocyte differentiation. PLoS One 4, e8190.

Lyu, J., Joo, C.K., 2004. Wnt signaling enhances FGF2-triggered lens fiber cell differentiation. Development 131, 1813–1824.

Mei, H., Gonzalez, S., Deng, S.X., 2012. Extracellular matrix is an important component of limbal stem cell niche. J. Funct. Biomater. 3, 879–894.

Mei, H., Nakatsu, M.N., Baclagon, E.R., Deng, S.X., 2014. Frizzled 7 maintains the undifferentiated state of human limbal stem/progenitor cells. Stem Cells 32, 938–945.

Moore, K.A., Lemischka, I.R., 2006. Stem cells and their niches. Science 311, 1880–1885.

Morgan, D.O., 1997. Cyclin-dependent kinases: engines, clocks, and microprocessors. Annu. Rev. Cell Dev. Biol. 13, 261–291.

Moyes, K.W., Sip, C.G., Obenza, W., Yang, E., Horst, C., Welikson, R.E., Hauschka, S.D., Folch, A., Laflamme, M.A., 2013. Human embryonic stem cell-derived cardiomyocytes migrate in response to gradients of fibronectin and Wnt5a. Stem Cells Dev. 22, 2315–2325.

Muñoz, R., Moreno, M., Oliva, C., Orbenes, C., Larraín, J., 2006. Syndecan-4 regulates non-canonical Wnt signalling and is essential for convergent and extension movements in Xenopus embryos. Nat. Cell Biol. 8, 492–500.

Nakatsu, M.N., Ding, Z., Ng, M.Y., Truong, T.T., Yu, F., Deng, S.X., 2011. Wnt/β-catenin signaling regulates proliferation of human cornea epithelial stem/progenitor cells. Invest. Ophthalmol. Vis. Sci. 52, 4734–4741.

Nakatsu, M.N., Vartanyan, L., Vu, D.M., Ng, M.Y., Li, X., Deng, S.X., 2013. Preferential biological processes in the human limbus by differential gene profiling. PLoS One 8, e61833.

Nusse, R., Fuerer, C., Ching, W., Harnish, K., Logan, C., Zeng, A., ten Berge, D., Kalani, Y., 2008. Wnt signaling and stem cell control. Cell Res. 18, 523–527.

Ohkawara, B., Yamamoto, T.S., Tada, M., Ueno, N., 2003. Role of glypican 4 in the regulation of convergent extension movements during gastrulation in Xenopus laevis. Development 130, 2129–2138.

Ouyang, H., Xue, Y., Lin, Y., Zhang, X., Xi, L., Patel, S., Cai, H., Luo, J., Zhang, M., Zhang, M., Yang, Y., Li, G., Li, H., Jiang, W., Yeh, E., Lin, J., Pei, M., Zhu, J., Cao, G., Zhang, L., Yu, B., Chen, S., Fu, X.D., Liu, Y., Zhang, K., 2014. WNT7A and PAX6 define corneal epithelium homeostasis and pathogenesis. Nature 511, 358–361.

Pimton, P., Sarkar, S., Sheth, N., Perets, A., Marcinkiewicz, C., Lazarovici, P., Lelkes, P.I., 2011. Fibronectin-mediated upregulation of α5β1 integrin and cell adhesion during differentiation of mouse embryonic stem cells. Cell Adh. Migr. 5, 73–82.

Reya, T., Clevers, H., 2005. Wnt signalling in stem cells and cancer. Nature 434, 843–850.

Richardson, A., Wakefield, D., Di Girolamo, N., 2016. Fate mapping mammalian corneal epithelia. Ocul. Surf. 14, 82–99.

Samuel, M.S., Lopez, J.I., McGhee, E.J., Croft, D.R., Strachan, D., Timpson, P., Munro, J., Schröder, E., Zhou, J., Brunton, V.G., Barker, N., Clevers, H., Sansom, O.J., Anderson, K.I., Weaver, V.M., Olson, M.F., 2011. Actomyosin-mediated cellular tension drives increased tissue stiffness and beta-catenin activation to induce epidermal hyperplasia and tumor growth. Cancer Cell 19, 776–791.

Sánchez-Solana, B., Laborda, J., Baladrón, V., 2012. Mouse resistin modulates adipogenesis and glucose uptake in 3T3-L1 preadipocytes through the ROR1 receptor. Mol. Endocrinol. 26, 110–127.

Schlötzer-Schrehardt, U., Dietrich, T., Saito, K., Sorokin, L., Sasaki, T., Paulsson, M., Kruse, F.E., 2007. Characterization of extracellular matrix components in the limbal epithelial stem cell compartment. Exp. Eye Res. 85, 845–860.

Schlötzer-Schrehardt, U., Kruse, F.E., 2005. Identification and characterization of limbal stem cells. Exp. Eye Res. 81, 247–264.

Shi, J., Wu, X., Surma, M., Vemula, S., Zhang, L., Yang, Y., Kapur, R., Wei, L., 2013. Distinct roles for ROCK1 and ROCK2 in the regulation of cell detachment. Cell Death Dis. 4, e483.

Shortt, A.J., Secker, G.A., Munro, P.M., Khaw, P.T., Tuft, S.J., Daniels, J.T., 2007. Characterization of the limbal epithelial stem cell niche: novel imaging techniques permit in vivo observation and targeted biopsy of limbal epithelial stem cells. Stem Cells 25, 1402–1409.

Shroff, K., Pearce, T.R., Kokkoli, E., 2012. Enhanced integrin mediated signaling and cell cycle progression on fibronectin mimetic peptide ampliphile monolayers, Langmuir 28, 1858–1865.

Singh, P., Schwarzbauer, J.E., 2012. Fibronectin and stem cell differentiation - lessons from chondrogenesis. J. Cell Sci. 125, 3703–3712.

Stump, R.J., Ang, S., Chen, Y., von Bahr, T., Lovicu, F.J., Pinson, K., de Iongh, R.U., Yamaguchi, T.P., Sassoon, D.A., McAvoy, J.W., 2003. A role for Wnt/beta-catenin signaling in lens epithelial differentiation. Dev. Biol. 259, 48–61.

Uysal-Onganer, P., Kypta, R.M., 2012. Wnt11 in 2011 - the regulation and function of a non-canonical Wnt. Acta Physiol. (Oxf). 204, 52–64.

Villegas, S.N., Rothová, M., Barrios-Llerena, M.E., Pulina, M., Hadjantonakis, A.K., Le Bihan, T., Astrof, S., Brickman, J.M., 2013. PI3K/Akt1 signalling specifies foregut precursors by generating regionalized extra-cellular matrix. Elife 2, e00806.

Woods, A., Couchman, J. R., 2001. Syndecan-4 and focal adhesion function. Curr. Opin. Cell Biol. 13, 578–583.

Yamanaka, H., Nishida, E., 2007. Wnt11 stimulation induces polarized accumulation of Dishevelled at apical adherens junctions through Frizzled7. Genes Cells 12, 961–967.

Yoneda, A., Multhaupt, H.A., Couchman, J.R., 2005. The rho kinases I and II regulate different aspects of myosin II activity. J. Cell Biol. 170, 443–453.

Yoneda, A., Ushakov, D., Multhaupt, H.A., Couchman, J.R., 2007. Fibronectin matrix assembly requires distinct contributions from rho kinases I and -II. Mol. Biol. Cell 18, 66–75.

Zhang, C., Zhang, S., Zhang, Z., He, J., Xu, Y., Liu, S., 2014. ROCK has a crucial role in regulating prostate tumor growth through interaction with c-Myc. Oncogene 33, 5582–5591.

Zhang, S., Tang, Q., Xu, F., Xue, Y., Zhen, Z., Deng, Y., Liu, M., Chen, J., Liu, S., Qiu, M., Liao, Z., Li, Z., Luo, D., Shi, F., Zheng, Y., Bi, F., 2009. RhoA regulates G1-S progression of gastric cancer cells by modulation of multiple INK4 family tumor suppressors. Mol. Cancer Res. 7, 570–580.

Figure captions

Fig. 1. Fibronectin (FN) promotes proliferation of rabbit limbal epithelial stem cells (rLESCs). (A): rLESC proliferation was higher in the 12.5 μg/cm^2 FN treatment [FN(12.5)] group than in the other groups at 3 h and 24 h, whereas proliferation significantly decreased in the FN-knockdown (FN-Kd) group, which was rescued after adding FN. (B): Ki67 staining showing a higher Ki67-positive cell proportion in the FN(12.5) rLESCs at 24 h. (C): The proportion of Ki67-positive cells was calculated, which was in accordance with the light microscopy results. (D): Cell doubling times were analyzed for each group. The doubling time in the FN(12.5) rLESCs was obviously shorter than those in the other groups. Ctrl, control (rLESCs cultured on plastic plates without treatment). Vehicle-Kd, an shRNA without targeting any known genes as a negative control for knockdown experiments. * $p < 0.05$, ** $p < 0.01$, one-way ANOVA and two-tailed *t* test.

Fig. 2. Fibronectin (FN) accelerates cell cycle progression of rabbit limbal epithelial stem cells (rLESCs). (A): Cell cycle analysis at 12 h showed a higher proportion of cells in the S phase in the 12.5 μg/cm^2 FN treatment [FN(12.5)] group than in the control group; however, the proportion of cells in the S phase significantly decreased when FN was knocked down. Moreover, the proportion of cells in S phase was significantly higher in the FN-knockdown (FN-Kd) group after treatment with FN than in the FN-Kd group. (B): The percentages of cells in G1, S, and G2/M phases from each group. Ctrl, control (rLESCs cultured on plastic plates without treatment). Vehicle-Kd, an shRNA without targeting any known genes as a negative control for knockdown experiments. ** $p < 0.01$, one-way ANOVA.

Fig. 3. Analysis of differentially expressed genes (DEGs) and KEGG pathways from 12.5 μg/cm^2 fibronectin treatment [FN(12.5)] and FN-knockdown (FN-Kd) groups of rabbit limbal epithelial stem cells (rLESCs). (A): Volcano plot of the expression profiles of 9834 DEGs between FN(12.5) *versus* FN-Kd groups. The red points represent upregulated DEGs (4894 genes) with statistical significance and the green points indicate downregulated DEGs (4940 genes). (B):

KEGG pathway analysis of DEGs between FN(12.5) *versus* FN-Kd groups showed enrichment in cell cycle, Hippo signaling, TNF signaling, MAPK signaling, mTOR signaling, signaling pathways that regulate stem cell pluripotency, TGF-beta signaling, VEGF signaling, ECM-receptor interaction, Ras signaling, Wnt signaling, cGMP-PKG signaling, PI3K-Akt signaling, Notch signaling, NF-kappa B signaling, and Hedgehog signaling. (C): Heatmap depicting DEGs from the FN-Kd, FN(12.5), and control groups. FN affected the expression of Wnt- and cell cycle-related genes. Differential expression analysis revealed that, compared with the FN-Kd group, the expression levels of Wnt family members *Wnt4* and *Wnt11*, Wnt pathway-related genes *Fzd1*, *Fzd7*, *Fzd9*, *RhoA*, *ROCK1*, *ROCK2*, *Ror1*, *Ryk*, and *Gpc4*, and cell cycle-related genes *CDK2*, *CDK4*, *CDK6*, *cyclin D1*, *cyclin D3*, *cyclin E1*, and *cyclin E2* were significantly upregulated in the FN(12.5) group, whereas $p21^{Cip1}$ and $p27^{Kip1}$ expressions were downregulated. In addition, rLESC marker ATP-binding cassette sub-family G member 2 (*ABCG2*) and transcription factor *Myc* were expressed at higher levels in the FN(12.5) group than the FN-Kd group. Ctrl, control (rLESCs cultured on plastic plates without treatment).

Fig. 4. Wnt11 promotes rabbit limbal epithelial stem cells (rLESCs) proliferation and the maintenance of stemness. Small interfering RNAs (siRNAs) were used to independently target *Wnt4* (siWnt4) and *Wnt11* (siWnt11) after rLESCs were treated with 12.5 μg/cm^2 fibronectin [FN(12.5)]. (A): Ki67-positivity decreased after siWnt4 transfection compared with that of the control group, but these differences were not significant. However, this parameter significantly decreased after siWnt11 treatment. (B): Quantitative reverse transcription PCR revealed that either Wnt4 or Wnt11 ablation can induce the differentiation of rLESCs, in which *cytokeratin 3* (*CK3*) was expressed abundantly but ATP-binding cassette sub-family G member 2 (*ABCG2*) and *ΔNp63* expressions were decreased. (C): The same trends were also found via immunofluorescence. Ctrl, control (rLESCs cultured on plastic plates without treatment). Vehicle, scramble-transfected control rLESCs. * $p < 0.05$, ** $p < 0.01$, two-tailed *t* test.

Fig. 5. Interactions between Wnt11 and Fzd7 result in a switch to non-canonical Wnt signaling in rabbit limbal epithelial stem cells (rLESCs). (A): Western blot analysis of

co-immunoprecipitated cells overexpressing FLAG-tagged Wnt11 and the HA-tagged ectodomain of Fzd7 in HEK293T cells. (B): Nuclear extracts western blot analysis of β-catenin in the rLESCs pretreated with 12.5 μg/cm^2 fibronectin [FN(12.5)] and 20 ng/ml Wnt3a, respectively. Histone H3 was used as loading control. (C): Histogram depicting the ratios of target protein to Histone H3 intensity; the corresponding control groups were set as 1 arbitrary unit. (D): TCF/LEF1 luciferase assay demonstrating that FN treatment does not enhance canonical Wnt signaling [control *versus* positive (20 ng/ml Wnt3a) groups]. * $p < 0.05$, ** $p < 0.01$, one-way ANOVA.

Fig. 6. Fibronectin (FN) modulates specific cell cycle-regulatory proteins to promote rabbit limbal epithelial stem cell (rLESC) proliferation via ROCK1 and ROCK2. (A): Western blot analysis of rLESC treated with 12.5 μg/cm^2 FN [FN(12.5)]. The FN(12.5) group showed upregulated expression of ROCK1, ROCK2, cyclin D1, cyclin D3, cyclin E1, cyclin E2, CDK2, CDK4, and CDK6, but downregulated expression of the CDK inhibitors (CDKIs) p21^{Cip1} and p27^{Kip1}. The ROCK inhibitor GSK429286A downregulated the cyclin and CDK expression, and upregulated the CDKI expression. siRNA-mediated targeting of either *ROCK1* or *ROCK2* showed similar effects as those of the inhibitor in rLESCs. (B): Histogram depicting the ratios of target protein to GAPDH intensity; the corresponding control groups were set as 1 arbitrary unit. Ctrl, control (rLESCs cultured on plastic plates without treatment). GSK, rLESCs treated with 50 μM GSK429286A for 48 h. siROCK1, rLESCs transfected with siRNA targeting *ROCK1* gene. siROCK2, rLESCs transfected with siRNA targeting *ROCK2* gene. * $p < 0.05$, ** $p < 0.01$ *versus* control group, two-tailed *t* test.

Fig. 7. Schematic diagram shows the regulatory effect of the Wnt11/Fzd7/ROCK pathway on G1/S transition in fibronectin (FN)-treated rabbit limbal epithelial stem cells (rLESCs). FN enhanced the interactions between Wnt11 and Fzd7; Ror1, Ryk, and Gpc4 are also involved in this process. GDP bound to RhoA is replaced by GTP, which further activates ROCK1 and ROCK2. ROCK1/2 activation elevates the expression of cyclin D1, cyclin D3, cyclin E1, cyclin E2, CDK2, CDK4, and CDK6—possibly by upregulating the phosphorylation of the transcription factor Myc—to enhance cell proliferation by promoting G1/S transition.

Supplemental figure captions

Supplemental Fig. 1. Proliferation and differentiation of rabbit limbal epithelial stem cells (rLESCs) after treatment with fibronectin (FN) at different concentrations. (A): Light microscopy results showing that 0.25, 2.5, 5.0, and 12.5 μg/cm^2 FN increased rLESC proliferation in a concentration-dependent manner, whereas 25 μg/cm^2 FN showed no significant effects compared with that of the control group. (B): Ki67 staining results were consistent with those of light microscopy. A FN concentration of 12.5 μg/cm^2 appeared to exert the most significant effects; therefore, we chose this concentration for further experiments. (C): Immunostaining results suggested that FN can maintain high expression levels of ATP-binding cassette sub-family G member 2 (ABCG2) and ΔNp63—identified as the specific markers in limbal stem cells. In contrast, the differentiation marker cytokeratin 3 (CK3)—known as a corneal epithelial cell marker—was only marginally expressed. Moreover, similar results were also found via (D) quantitative reverse transcription PCR and (E) western blotting. (F): Histograms depicting the ratios of target protein to GAPDH intensities; the corresponding control groups were set as 1 arbitrary unit. Ctrl, control (rLESCs cultured on plastic plates without treatment). * $p < 0.05$, ** $p < 0.01$ *versus* control group, two-tailed *t* test.

Supplemental Fig. 2. Rabbit limbal epithelial stem cells (rLESCs) with fibronectin (FN) knockdown were prepared using short hairpin RNA (shRNA). (A): Western blot analysis indicated that FN expression declined significantly in the FN-Kd1 and FN-Kd2 groups compared with that of the control group. (B): Histograms depicting the ratios of target protein to β-actin intensities; the corresponding control groups were set as 1 arbitrary unit. The FN expression level in the FN-Kd1 rLESCs significantly decreased by approximately 96% than the control. Therefore, FN-Kd1 rLESCs were used for subsequent experiments and termed FN-Kd rLESCs. (C): Immunostaining demonstrated decreased FN expression in the FN-Kd rLESCs compared with that of the control group. And there was no significant difference in FN expression between the control and vehicle-Kd cells. (D): Phosphatidylserine (PS) externalization experiments were conducted to detect apoptosis using flow cytometry after FN knockdown; FN knockdown did not induce apoptosis. (E): Quantitative reverse transcription PCR revealed that FN knockdown significantly downregulated the expression levels of *Wnt11*, *frizzled7* (*Fzd7*), Rho-associated kinase 1 (*ROCK1*), and the rLESC markers including ATP-binding cassette sub-family G member 2 (*ABCG2*) and *ΔNp63*, while upregulated *β-catenin* and the differentiation marker *cytokeratin 3* (*CK3*). The expression levels of these genes from the vehicle-Kd rLESCs had no significant difference from those of control. Ctrl, control (rLESCs cultured on plastic plates without treatment). Vehicle-Kd: scramble-transfected control rLESCs using shRNA. * $p < 0.05$, ** $p < 0.01$, one-way ANOVA.

Supplemental Fig. 3. Cluster analysis of differentially expressed genes (DEGs) from 12.5 μg/cm^2 fibronectin treatment [FN(12.5)], FN-knockdown (FN-Kd), and control groups. The samples from the FN(12.5), FN-Kd, and control groups were detected to perform a heatmap for cluster analysis of the DEGs. Red indicates upregulated genes and blue indicates downregulated genes. Ctrl, control (rLESCs cultured on plastic plates without treatment).

Supplemental Fig. 4. ROCK1 and ROCK2 are involved in signaling via RhoA after enhancing the interaction between Wnt11 and Fzd7 in fibronectin (FN)-treated rabbit limbal epithelial stem cells (rLESCs). (A): Western blot analysis indicated that expression levels of RhoA, ROCK1, and ROCK2 were upregulated after addition of recombinant Wnt11 (10 ng/ml) for 24 h, whereas the expression levels decreased after addition *Wnt11*-specific siRNA; this was rescued by treatment with recombinant Wnt11 (10 ng/ml). (B): Histograms depicting the ratios of RhoA, ROCK1, or ROCK2 to GAPDH intensity; the corresponding control groups were set as 1 arbitrary unit. ** $p < 0.01$, one-way ANOVA.

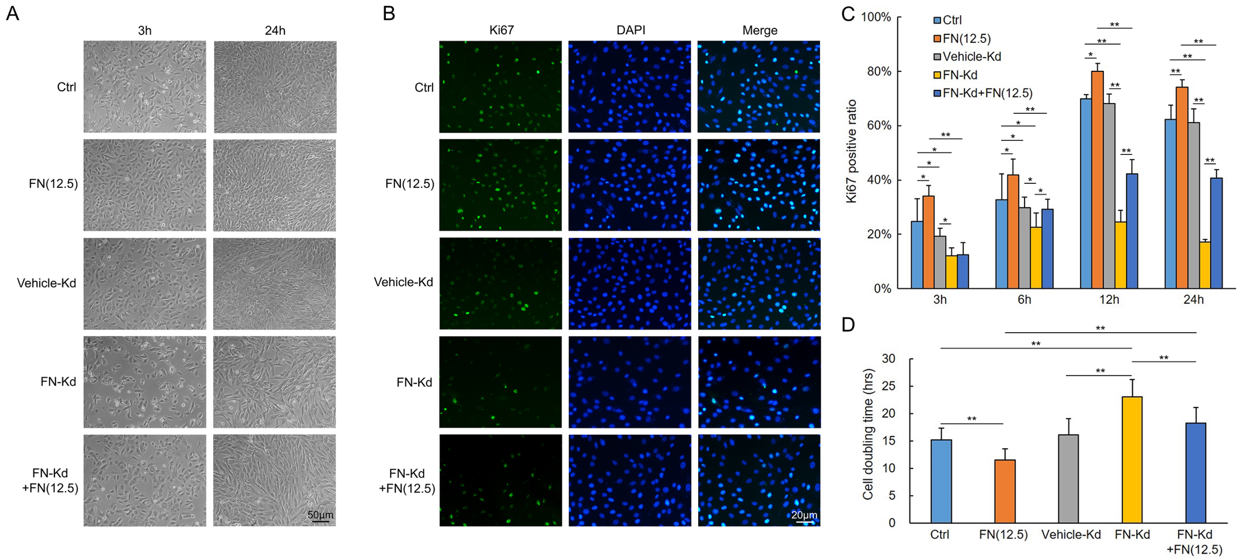
A
3h
24h
Ctrl
FN(12.5)
Vehicle-Kd
FN-Kd
FN-Kd
+FN(12.5)
50μm
B
Ki67
DAPI
Merge
Ctrl
FN(12.5)
Vehicle-Kd
FN-Kd
FN-Kd
+FN(12.5)
20μm
C
Ctrl
FN(12.5)
Vehicle-Kd
FN-Kd
FN-Kd+FN(12.5)
Ki67 positive ratio
100%
80%
60%
40%
20%
0%
3h
6h
12h
24h
D
Cell doubling time (hrs)
30
25
20
15
10
5
0
Ctrl
FN(12.5)
Vehicle-Kd
FN-Kd
FN-Kd
+FN(12.5)

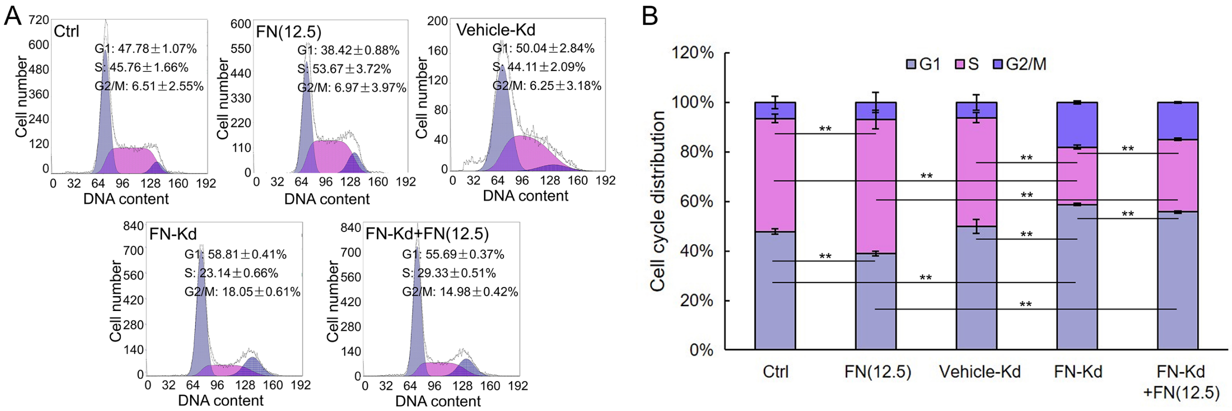
A
Ctrl
G1: 47.78±1.07%
S: 45.76±1.66%
G2/M: 6.51±2.55%
FN(12.5)
G1: 38.42±0.88%
S: 53.67±3.72%
G2/M: 6.97±3.97%
Vehicle-Kd
G1: 50.04±2.84%
S: 44.11±2.09%
G2/M: 6.25±3.18%
FN-Kd
G1: 58.81±0.41%
S: 23.14±0.66%
G2/M: 18.05±0.61%
FN-Kd+FN(12.5)
G1: 55.69±0.37%
S: 29.33±0.51%
G2/M: 14.98±0.42%
Cell number
DNA content
B
G1 S G2/M
Cell cycle distribution
Ctrl
FN(12.5)
Vehicle-Kd
FN-Kd
FN-Kd +FN(12.5)

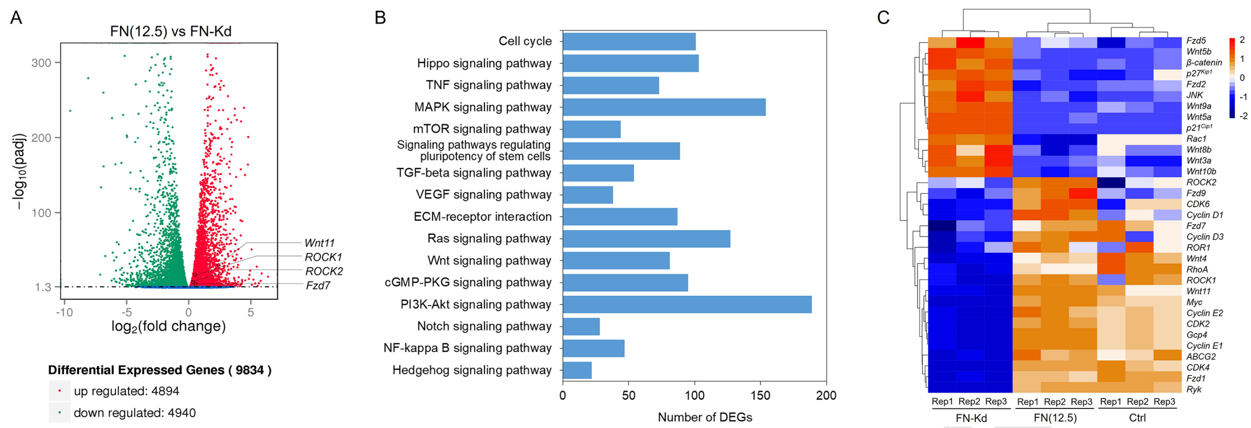
A
FN(12.5) vs FN-Kd
−log10(padj)
log2(fold change)
Wnt11
ROCK1
ROCK2
Fzd7
Differential Expressed Genes (9834)
up regulated: 4894
down regulated: 4940
B
Cell cycle
Hippo signaling pathway
TNF signaling pathway
MAPK signaling pathway
mTOR signaling pathway
Signaling pathways regulating pluripotency of stem cells
TGF-beta signaling pathway
VEGF signaling pathway
ECM-receptor interaction
Ras signaling pathway
Wnt signaling pathway
cGMP-PKG signaling pathway
PI3K-Akt signaling pathway
Notch signaling pathway
NF-kappa B signaling pathway
Hedgehog signaling pathway
Number of DEGs
C
Rep1 Rep2 Rep3
FN-Kd
FN(12.5)
Ctrl

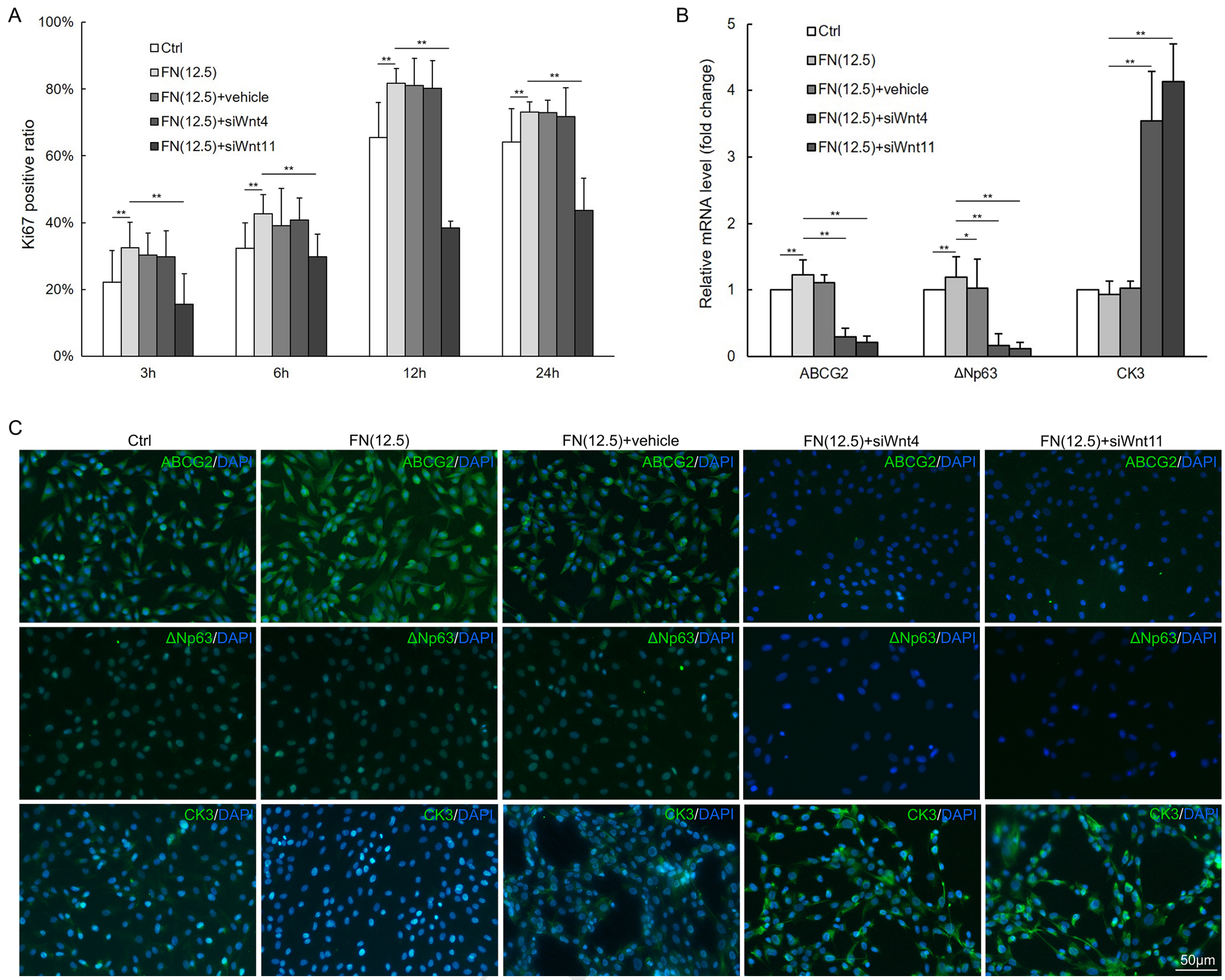
A
100%
80%
60%
40%
20%
0%
Ki67 positive ratio
Ctrl
FN(12.5)
FN(12.5)+vehicle
FN(12.5)+siWnt4
FN(12.5)+siWnt11
3h
6h
12h
24h
B
Relative mRNA level (fold change)
ABCG2
ΔNp63
CK3
C
Ctrl
FN(12.5)
FN(12.5)+vehicle
FN(12.5)+siWnt4
FN(12.5)+siWnt11
ABCG2/DAPI
ΔNp63/DAPI
CK3/DAPI
50μm

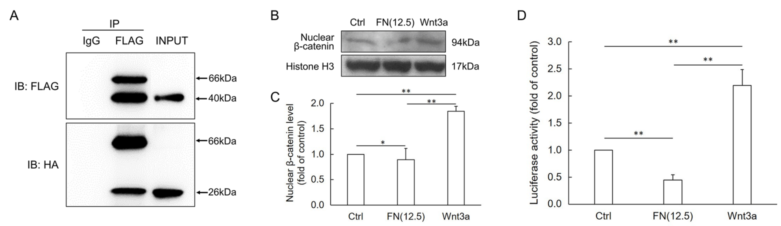
A
IP
IgG
FLAG
INPUT
IB: FLAG
IB: HA
66kDa
40kDa
66kDa
26kDa
B
Ctrl
FN(12.5)
Wnt3a
Nuclear β-catenin
Histone H3
94kDa
17kDa
C
Nuclear β-catenin level (fold of control)
Ctrl
FN(12.5)
Wnt3a
D
Luciferase activity (fold of control)
Ctrl
FN(12.5)
Wnt3a

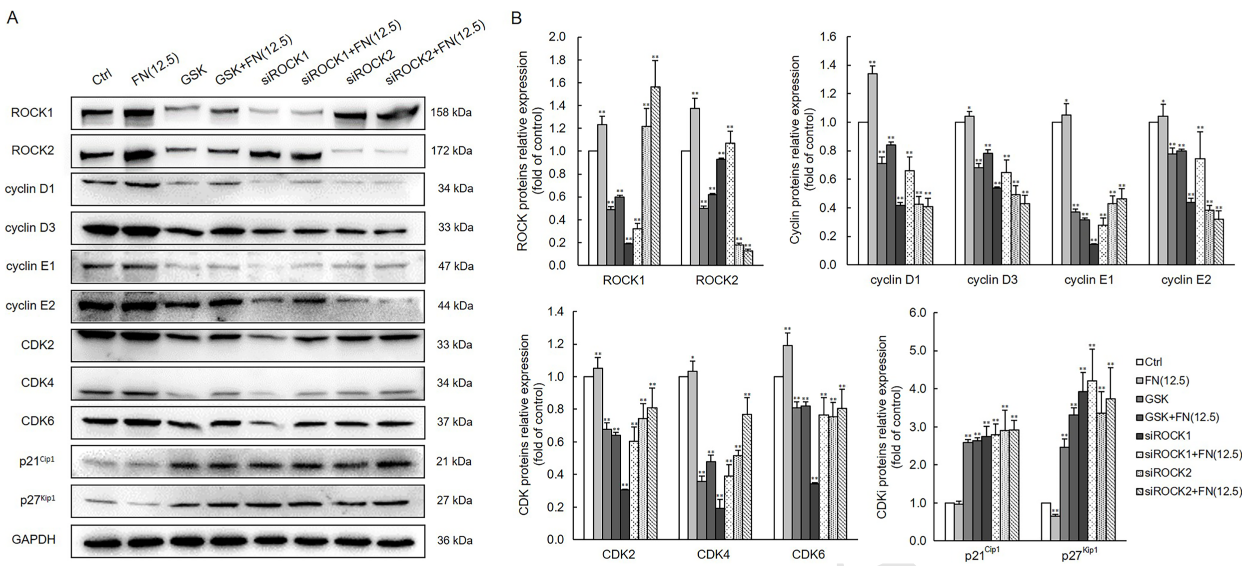
A
Ctrl
FN(12.5)
GSK
GSK+FN(12.5)
siROCK1
siROCK1+FN(12.5)
siROCK2
siROCK2+FN(12.5)
ROCK1
158 kDa
ROCK2
172 kDa
cyclin D1
34 kDa
cyclin D3
33 kDa
cyclin E1
47 kDa
cyclin E2
44 kDa
CDK2
33 kDa
CDK4
34 kDa
CDK6
37 kDa
p21Cip1
21 kDa
p27Kip1
27 kDa
GAPDH
36 kDa
B
ROCK proteins relative expression (fold of control)
ROCK1
ROCK2
Cyclin proteins relative expression (fold of control)
cyclin D1
cyclin D3
cyclin E1
cyclin E2
CDK proteins relative expression (fold of control)
CDK2
CDK4
CDK6
CDKi proteins relative expression (fold of control)
p21Cip1
p27Kip1
Ctrl
FN(12.5)
GSK
GSK+FN(12.5)
siROCK1
siROCK1+FN(12.5)
siROCK2
siROCK2+FN(12.5)

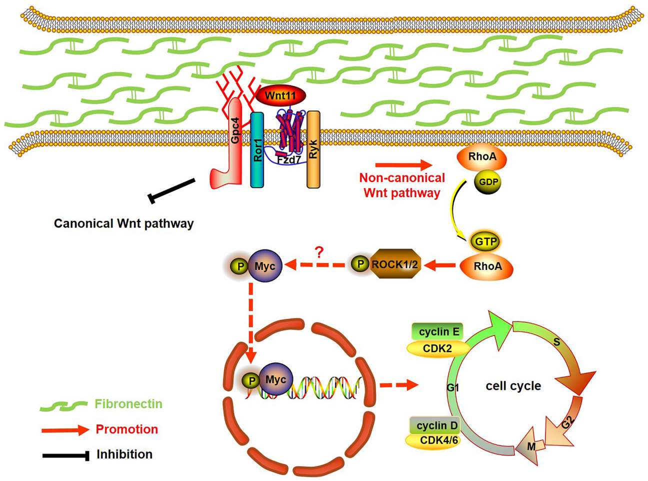

Wnt11
Gpc4
Ror1
Fz7
Ryk
RhoA
GDP
Non-canonical
Wnt pathway
Canonical Wnt pathway
GTP
RhoA
?
P
Myc
P
ROCK1/2
cyclin E
CDK2
S
P
Myc
G1
cell cycle
G2
M
cyclin D
CDK4/6
Fibronectin
Promotion
Inhibition

HIGHLIGHTS

- FN improves the self-renewal of rabbit limbal epithelial stem cells (rLESCs).
- rLESC proliferation is enhanced through modulating ROCK1/2 and cell cycle regulators.
- FN regulates rLESC self-renewal by stimulating the Wnt11/Fzd7/ROCK non-canonical Wnt pathway.